유체－구조물 상호작용이 원자로내부구조물의 동적응답에 미치는 영향

The Effect of Fluid-Structure Interaction on the Dynamic Response of Reactor Internals

정 명 조*
Jhung, Myung-Jo
박 찬 국**
Park, Chan-Kuk
황 원 걸***
Hwang, Won-Gul

요 약

원자로내부구조물은 유체속에 잠겨있기 때문에 동적해석시 이의 영향을 고려해야한다. 본 논문에서는 지진 및 배관파단에 대한 원자로내부구조물의 동적해석을 위한 비선형해석모델을 제시하였고 유체－구조물 상호작용의 효과를 고려하는 방법에 대하여 설명하였다. 실제 해석을 통하여 유체－구조물 상호작용이 원자로내부구조물의 응답에 미치는 영향을 조사한 결과 지진해석시에는 유체－구조물 상호작용을 나타내는 hydrodynamic coupling 항이 첨가됨으로써 높은 응답이 나왔으나, 배관파단시에는 이와 반대의 결과가 나왔다.

Abstract

Investigated in this paper is the effect of fluid-structure interaction between reactor internal components due to their immersion in a confining fluid on the dynamic responses. A non-linear mathematical model is developed for the dynamic analysis of the reactor internals, which includes lumped masses, stiffnesses and hydrodynamic couplings. The hydrodynamic mass matrix which characterizes the fluid-structure interaction is calculated. Also, the equations of motion containing hydrodynamic mass matrix are presented. The responses of the reactor internals due to seismic and pipe break excitations are obtained for the case of with- and without-hydrodynamic couplings and the different response characteristics are investigated.

* 정회원, 한국원자력연구소 원자로기계설계실 선임연구원
** 전남대학교 기계공학과 교수
*** 전남대학교 기계설계학과 교수

이 논문에 대한 토론을 1994년 6월 30일까지 본 학회에 보내주시면 1994년 12월호에 그 결과를 게재하겠습니다.

1. INTRODUCTION

The reactor internals include the core support barrel (CSB) assembly, the lower support structure (LSS) & ICI nozzle assembly, the core shroud, and the upper guide structure (UGS) assembly. The core support barrel is a right circular cylinder supported by a ring flange from a ledge on the reactor vessel. It carries the entire weight of the core. The lower support structure transmits the weight of the core to the core support barrel by means of a beam structure. The core shroud surrounds the core and minimizes the amount of bypass flow. The upper guide structure provides a flow shroud for the control element assemblies (CEAs), and limits upward motion of the fuel assemblies during pressure transients. Lateral snubbers are provided at the lower end of the core support barrel assembly. All of these reactor internal structures are immersed in a fluid and its fluid-structure interaction should be accounted for the calculation of dynamic responses under seismic and pipe break excitations.

This paper presents the methodology to account for the fluid-structure interaction effect on the dynamic responses of reactor internals and fuel, and also presents the mathematical model for the time history analysis of the reactor internals. The responses of reactor internals due to seismic and pipe break excitations are investigated.

2. THEORETICAL DEVELOPMENT

2.1 FORMULATION OF EQUATIONS

The general equations of motion for a base excited system can be written as

$$[M]\{\ddot{x}\}+[C]\{\dot{u}\}+[K]\{u\}=\{0\} \qquad (1)$$

where $[M]=[M_s]+[M_h]$: mass matrix

$[M_s]$: structural mass matrix

$[M_h]$: hydrodynamic mass matrix

$[C]$=damping matrix

$[K]$=stiffness matrix

$\{\ddot{x}\}$ =absolute acceleration

$\{\dot{u}\}$ =velocity relative to the base

$\{u\}$ =displacement relative to the base.

The structural mass plus hydrodynamic mass matrix $[M]$ for the n lumped mass is given by

$$\begin{bmatrix} (M_1+M_{11}) & -(M_{12}) & 0 & 0 & - & 0 & 0 \\ -(M_{12}) & (M_2+M_{22}) & 0 & 0 & - & 0 & 0 \\ 0 & 0 & (M_3+M_{33}) & -(M_{34}) & - & 0 & 0 \\ 0 & 0 & -(M_{34}) & (M_4+M_{44}) & - & 0 & 0 \\ - & - & - & - & - & - & - \\ - & - & - & - & - & - & - \\ 0 & 0 & 0 & 0 & - & (M_{n-1}+M_{n-1,n-1}) & -(M_{n-1,n}) \\ 0 & 0 & 0 & 0 & - & -(M_{n-1,n}) & (M_n+M_{n,n}) \end{bmatrix}$$

where M_i, i=1,n is a real mass at node i and M_{ij} are the hydrodynamic mass matrix components.

If subset of the motions are prescribed $\{u_b\}$, then equation (1) can be partitioned as follows :

$$\begin{bmatrix} M_{aa} & M_{ab} \\ M_{ba} & M_{bb} \end{bmatrix}\begin{Bmatrix} \ddot{x}_a \\ \ddot{x}_b \end{Bmatrix}+\begin{bmatrix} C_{aa} & C_{ab} \\ C_{ba} & C_{bb} \end{bmatrix}\begin{Bmatrix} \dot{u}_a \\ \dot{u}_b \end{Bmatrix}+\begin{bmatrix} K_{aa} & K_{ab} \\ K_{ba} & K_{bb} \end{bmatrix}\begin{Bmatrix} u_a \\ u_b \end{Bmatrix}=\begin{Bmatrix} 0 \\ p_b \end{Bmatrix} \qquad (2)$$

where the subscripts a and b denote mass points of two adjacent structues and $\{p_b\}$ is a set of forces which will result in the prescribed motions $\{u_b\}$.

2.2 CALCULATION OF MASS MATRIX

The equations of motion account for fluid-structure interaction between two adjacent structures, separated by a fluid-filled gap, and the fluid forces in equation (2) are evaluated applying a hydrodynamic mass matrix. The

mass matrix components are determined depending upon the axial boundary conditions at the ends of annulus and upon whether or not the coupling is 2 - or 3-dimensional.

The 3-dimensional theory accounts for the translation of both the inner and outer cylinders and specification of fluid axial boundary conditions at the ends of the annulus. The continuity equation at any instant of time can be written as :

$$\frac{\partial^2\phi}{\partial r^2}+\frac{1}{r}\frac{\partial^2\phi}{\partial\theta^2}+\frac{\partial^2\phi}{\partial z^2}=0 \qquad (3)$$

where, r, θ, z are polar coordinate system and ϕ is a velocity potential function. The fluid potential is evaluated by applying the fluid boundary conditions to the equation (3). The fluid boundary conditions in the axial direction are defined at $z=0$ and $z=L$. At these locations the boundary conditons define either an open end (i.e., zero pressure) or a closed end (i.e., zero velocity). The fluid boundary conditions at the structural boundaries are given in terms of the radial components of the structural translational velocities [1].

The fluid potential function is used to evaluate the fluid forces per unit length on each of the edjacent structures. The SHOCK code [2] discretizes the structures using a series of beams and nodes. Each node represents the mass properties of a segment of the structure. For example, consider the mass properties at node A_o and A_i are associated with the structureal length, L_2-L_1 (Fig.1). The hydrodynamic forces at nodes A_o and A_i are obtained from the fluid forces per unit length by integrating with respect to z from L_1 to L_2. Therefore, in terms of a 2×2 mass matrix, the hydrodynamic forces on nodes A_i and A_o over a segment, L, on a cylinder are

$$\begin{bmatrix} F_{A_i} \\ F_{A_o} \end{bmatrix}=\begin{bmatrix} m_{11} & m_{12} \\ m_{21} & m_{22} \end{bmatrix}\begin{bmatrix} \ddot{x}_i \\ \ddot{x}_o \end{bmatrix} \qquad (4)$$

where

$$m_{11}=2\rho aL\sum_m \frac{q_m\int_{L_1}^{L_2} z_m(z)\,dz}{m\Delta x_i}\left\{K_1'\left(\frac{m\pi b}{2L}\right)I_1\left(\frac{m\pi a}{2L}\right)-I_1'\left(\frac{m\pi b}{2L}\right)K_1\left(\frac{m\pi a}{2L}\right)\right\}$$

$$m_{12}=2\rho aL\sum_m \frac{h_m\int_{L_1}^{L_2} z_m(z)\,dz}{m\Delta x_o}\left\{-K_1'\left(\frac{m\pi a}{2L}\right)I_1\left(\frac{m\pi a}{2L}\right)+I_1'\left(\frac{m\pi b}{2L}\right)K_1\left(\frac{m\pi a}{2L}\right)\right\}$$

$$m_{21}=2\rho bL\sum_m \frac{q_m\int_{L_1}^{L_2} z_m(z)\,dz}{m\Delta x_i}\left\{-K_1'\left(\frac{m\pi b}{2L}\right)I_1\left(\frac{m\pi b}{2L}\right)+I_1'\left(\frac{m\pi b}{2L}\right)K_1\left(\frac{m\pi b}{2L}\right)\right\}$$

$$m_{22}=2\rho bL\sum_m \frac{h_m\int_{L_1}^{L_2} z_m(z)\,dz}{m\Delta x_o}\left\{K_1'\left(\frac{m\pi b}{2L}\right)I_1\left(\frac{m\pi b}{2L}\right)-I_1'\left(\frac{m\pi a}{2L}\right)K_1\left(\frac{m\pi b}{2L}\right)\right\}$$

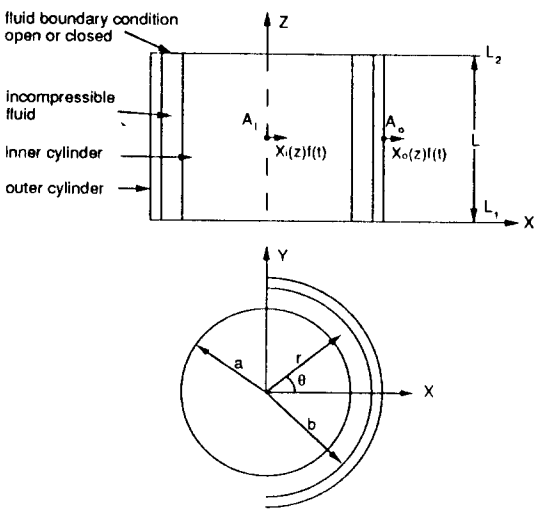

Fig. 1 Hydrodynamic mass representation

These equations form the basis for the evaluation of the complete hydrodynamic mass matrices, which are evaluated for the four practical cases in the reactor internals such as :

1) outer cylinder fixed ; closed-open fluid annulus,
2) closed-open fluid annulus,
3) contained mass of an outer cylinder with no inner cylinder,

4) outer cylinder fixed ; closed-closed fluid annulus.

3. DYNAMIC ANALYSES

3.1 MODEL DEVELOPMENT

The mathematical model of the reactor internals consists of lumped masses and elastic beam elements to represent the beam-like behavior of the internals, and non-linear elements to simulate the effects of gaps between components. Typical component gaps represented by non-linear elements are the core support barrel, pressure vessel snubber gap and core shroud guide lug gap. The gaps between the core shroud and core support barrel or the core support plate and core support barrel are sufficiently large that no contacting occurs. For every analysis performed, this assumption is verified by confirming that the relative deflections of components are in fact smaller than the existing gaps.

At appropriate locations within the reactor internals and core, nodes are chosen to lump the weights of the structure. The criterion for choosing the number and location of mass points is to provide for accurate representation of the dynamically significant modes of vibration for each of the components. For the beam element connecting two nodes, properties are calculated for moments of inertia, cross-sectional areas, effective shear areas, stiffnesses and length.

Stiffnesses for the complex structures such as flanges, snubber, hold-down ring and tube bank are determined by finite element analyses. Unit deflections and rotations are applied and the resulting reaction forces are calculated. These results are then used to derive the equivalent member properties for the structures.

The CSB upper region is modeled to account for the possible interactions between the CSB upper flange, UGS upper flange, hold-down ring and the reactor vessel(RV) ledge using the non-linear, hysteresis and friction elements. But if justified by analysis, it can be modeled as one mass point because the design basis pipe break size is small.

A typical coupled reactor internals and core model in the horizontal direction is shown in Fig.2. The actual arrangement and detail in the model may vary with the function of plant design, and the magnitude and nature of the pipe break excitation. For example, the loads on CEA guide tubes during an inlet break can be negligible because it is assumed that there is negligible crossflow at the outlet nozzle plenum for an inlet break. That's why the model of CEA guide tubes is represented by single beam element in the analysis of inlet pipe break.

It has been shown both analytically and experimentally that the immersion of a body in a dense-fluid medium lowers its natural frequency and significantly alters its vibratory response as compared to that in air [3]. The effect is more pronounced where the confining

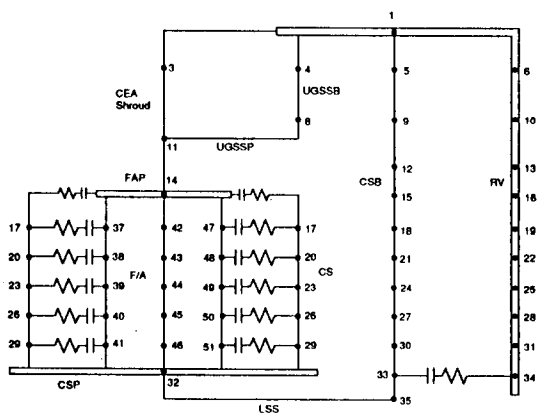

Fig. 2 Mathematical model of the reactor internals

boundaries of the fluid are in close proximity to the vibrating body as in the case of the reactor internals. The method of accounting for the effect of a surrounding fluid on a vibrating system has been to ascribe to the system additional or hydrodynamic mass. The hydrodynamic mass of an immersed system is a function of the dimensions of the real mass and the space between the real mass and confining boundary. Therefore, the effect of fluid-structure interaction between internal components due to their immersion in a confining fluid is considered. The hydrodynamic mass matrix is applied to the analytical model representing the reactor internal structures in the horizontal direction. Fluid-structure interaction is characterized by the full hydrodynamic mass matrix including the off-diagonal hydrodynamic coupling terms which will affect significantly the dynamic characteristic of the solid structure with narrow gap or annulus.

Hydrodynamic mass terms are calculated for the lumped mass model considering the solution of two concentric cylinders moving in fluid and including various boundary conditions associated with the fixity of the cylinders and the fluid flow in the axial direction. The potential flow theory is used for the formulation of fluid pressures developed in the annulus between the two concentric moving cylinders. The fluid pressure includes the effects of the beam deformation of the cylinders as well as the axial fluid flow in the annulus. The hydrodynamic pressures are converted to added-mass (diagonal) and coupling-mass (hydrocoupling) terms to be added to the mass matrix of the lumped mass model.

The fluid-structure interaction of the core region is determined experimentally. The complex configuration of fuel assemblies, closed spaced fuel rod arrays, and fuel assembly internal hysteresis and friction preclude a formal evaluation of the hydrodynamic mass matrix. Test data is used to obtain the net effect of fluid-structure interaction on the fuel assemblies' natural frequencies. The fuel assembly hydrodynamic added mass is then evaluated to yield natural frequencies consistent with the test data [4].

3.2 RESPONSES

Structures and equipment in a nuclear power plant are required to be designed or qualified to resist the combined effects of a large number of loads including static loads (e.g., dead weight, pressure loads and temperature loads) and multiple dynamic loads. The dynamic loads are either transmitted directly to the entire primary structure of a nuclear power plant in the form of vibratory loads or they may be generated within the primary structures due to plant conditions. The dynamic loads which are considered in the design and evaluation include those from natural phenomena like earthquakes, and from plant conditions which are either postulated to occur, for example, the pipe break loads, or those that trigger automatically to prevent accidents within the plant, like the Safety Depressurization System Valve actuation loads.

The seismic design loads may be computed based on either an actual earthquake record calibrated for a given plant site, or an artificial earthquake computable with USNRC Regulatory Guide 1.60 [5] spectra. A site-specific or natural earthquake is generally narrow frequency band earthquake as compared to one generated from a Regulatory Guide 1.60 spectra. The frequency band of the earthquake depends on the plant site. For the Yonggwang Nuclear Power Plant Unit 3 and 4

in Korea, the design basis earthquake has maximum free field horizontal ground accelerations at the foundation level of 0.20g for the safe shutdown earthquake (SSE) and 0.10g for operating basis earthquake (OBE). The maximum vertical ground accelerations at the foundation level are 0.13g for the SSE and 0.067g for the OBE. Based on this information, the architect engineer generated base motions and one of building analysis results is support motions of the reactor coolant system. Reactor vessel motions are obtained from the reactor coolant system analysis in which a very simplified model of the reactor internals and core is used. It is used as an input to the coupled model of the reactor internals and core.

The pipe break loads which are significant to the design of nuclear power plant structures and equipments are produced by a postulated design basis break. In the recent design of nuclear power plants, main coolant loop double ended guillotine breaks are eliminated from the design basis because of leak-before-break (LBB) concept [6]. Instead, branch line pipe breaks are considered as one of the Level D service loadings. Among the branch line pipe breaks postulated, LBB evaluation is performed for piping systems with a diameter of 10 inches or over and it is anticipated that pipe breaks with a diameter of 10 inches or over be no more considered as design basis. In this case, only the 3 inch pressurizer spray line nozzle break remains in the design basis in the primary side. As the pipe break size becomes smaller, the reactor vessel motions are negligible [7] and the only forcing terms are CSB forces associated with asymmetric pressurization of containment subcomparments due to pipe break accidents. The exciting time histories are shown in Fig.3 and Fig.4, which are the acceleration time histories of RV flange and snubber for earthquake and the CSB force time history for pipe break, respectively.

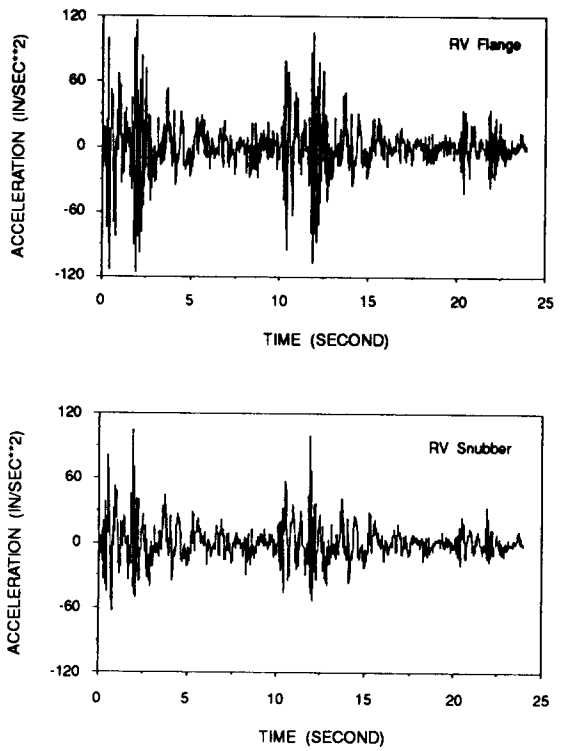

Fig. 3 Acceleration time histories of RV flange and snubber for earthquake

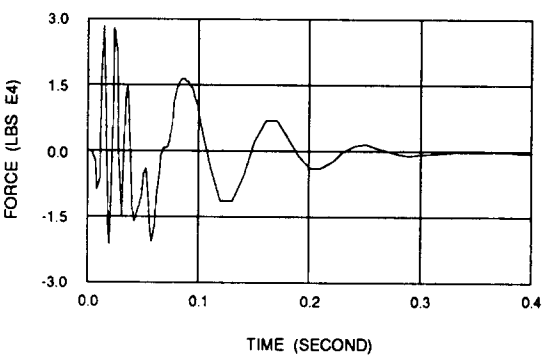

Fig. 4 CSB force time history for pipe break

4. RESULTS AND DISCUSSION

The results of analysis consist of minimum and maximum values of shears and moments of each component which will be used for design loads, and motions for fuel alignment plate and core support plate which will be used for the detailed core analysis.

The maximum loads of each component are summarized in Tables 1 and 2. The comparison of the responses for the seismic excitation shows that the higher responses are obtained in the with-hydrodynamic coupling case than without-case. This indicates that the RV motions, which are used as forcing functions, are transmitted by the RV flange and snubber as well as hydrodynamic couplings and generate a large displacement of overall internal structures. But the pipe break responses show the opposite characteristcs, or the loads for without-hydrodynamic coupling case are higher than with-case. This is explained by the fact that CSB forces are transmitted through hydrodynamic coupling terms to RV which is very stiff comparing with the reactor internal structures.

Table 1. Maximum loads of reactor internals for seismic exciation

Component	SHEAR (ℓ bxE5)		MOMENT (in-ℓ bxE5)	
	w/	w/o	w/	w/o
CSB Upper Flange	6.35	2.49	44.39	39.74
CSB Upper Cylinder	6.35	2.49	43.47	32.89
CSB Nozzle Cylinder	3.44	1.91	37.96	25.63
CSB Center Cylinder	4.40	1.48	33.22	15.48
CSB Lower Cylinder	4.33	1.26	41.54	19.21
CSB Lower Flange	5.80	3.10	47.46	21.34
CSB Snubber	3.86	2.96	–	–
LSS	4.91	2.65	47.79	20.48
Core Shroud	4.18	1.94	41.41	17.73
UGS Upper Flange	6.49	1.44	48.54	18.54
UGS Lower Flange	1.35	1.24	7.43	3.10
CEA Guide Tube	1.20	.60	7.01	3.31
CEA Shroud Assembly	.90	.70	3.81	2.93

Table 2. Maximum loads of reactor internals for pipe break exciation

Component	SHEAR (ℓ bxE5)		MOMENT (in-ℓ bxE5)	
	w/	w/o	w/	w/o
CSB Upper Flange	.20	.38	2.10	8.14
CSB Upper Cylinder	.20	.37	1.85	6.67
CSB Nozzle Cylinder	.19	.30	1.64	5.18
CSB Center Cylinder	.15	.25	.90	2.86
CSB Lower Cylinder	.09	.25	.74	.38
CSB Lower Flange	.10	.26	.86	.78
CSB Snubber	.00	.00	–	–
LSS	.07	.17	.86	.82
Core Shroud	.09	.08	.76	.59
UGS Upper Flange	.20	.19	1.42	2.42
UGS Lower Flange	.05	.13	.98	.62
CEA Guide Tube	.01	.04	.02	.12
CEA Shroud Assembly	.01	.05	.10	.50

The relative displacement and/or shear force time histories of RV to CSB snubber (Figs.5, 6 and 7) indicate that the hydrodynamic coupling terms act as a snubber

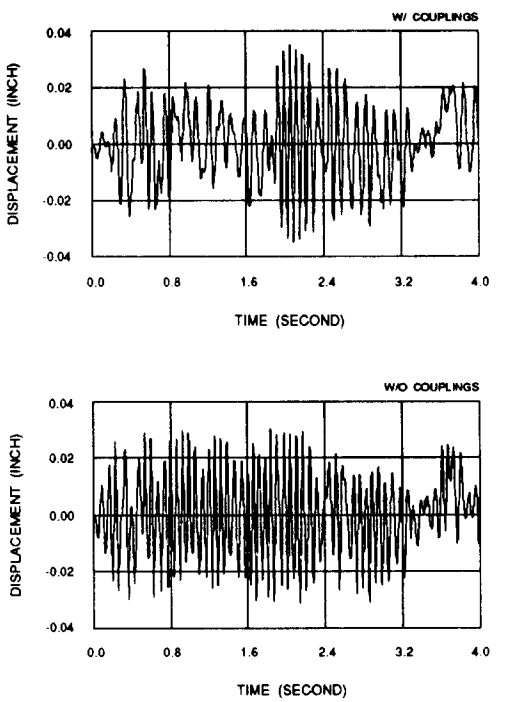

Fig. 5 Relative displacement time histories of CSB snubber to RV for earthquake

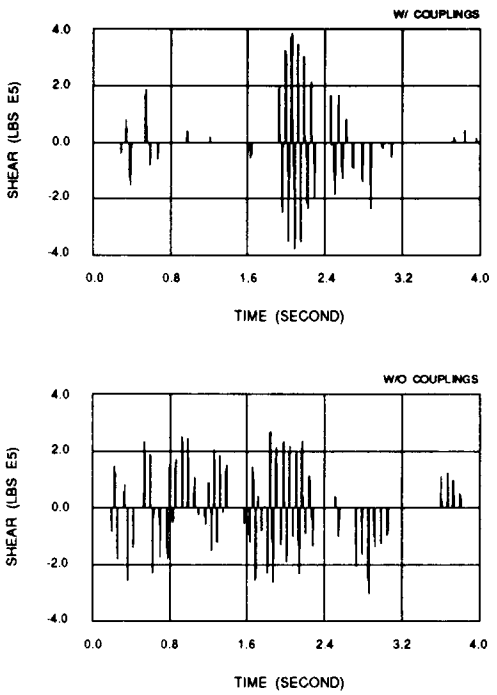

Fig. 6 Shear force time histories of CSB snubber to RV for earthquake

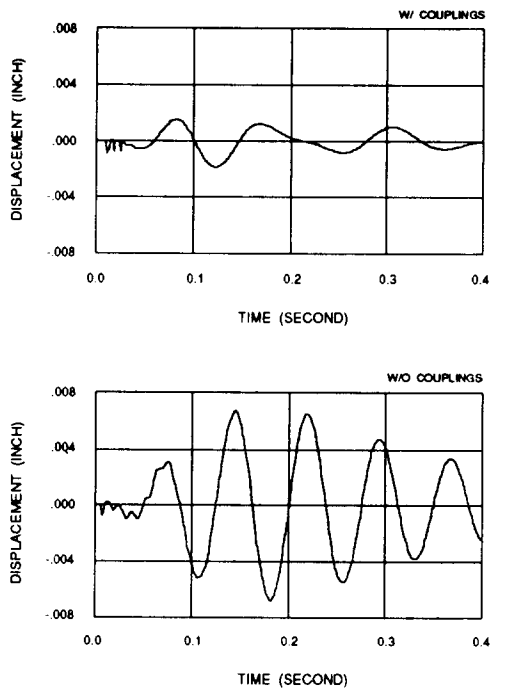

Fig. 7 Relative displacement time histories of CSB snubber to RV for pipe break

which restraints the motion of the CSB. The degree of this snubber effect by hydrodynamic couplings depends on the location of the forcing functions which are applied to the reactor internals.

5. CONCLUSIONS

The effect of fluid-structure interaction on the dynamic response of reactor internals has been investigated. The hydrodynamic mass matrix which characterizes the fluid effect was developed for the dynamic analysis of the reactor internals. The responses of the reactor internals for seismic and pipe break excitations were obtained for the case of with- and without-hydrodynamic couplings. It has been found that seismic responses are higher for with-hydrodynamic couplings case than without-case, but the pipe break responses show the opposite characteristics.

NOMENCLATURE

a : outer radius of inner cylinder
b : inner radius of outer cylinder
L : total length of cylinder
m_{ij} : hydrodynamic mass matrix components
x_i, x_o : translation of inner and outer cylinders
m : a set of integers chosen to satisfy specific axial fluid boundary conditions
$z_m(z)$: a series expansion function of conditions x_i, x_o
h_m, q_m : two sets of series expansion coefficients
I_1, K_1 : modified Bessel function of the first and second kind, of order one

Δ : $K_1'(\frac{m\pi a}{2L})I_1'(\frac{m\pi b}{2L}) - I_1'(\frac{m\pi a}{2L})K_1'(\frac{m\pi b}{2L})$

ρ : fluid mass density

REFERENCES

1. M.J. Jhung, et al., "The Effect of Fluid/Structure Interaction on the Reactor Internals Responses for Seismic and Pipe Break Excitations," ASME PVP-Vol.253, The American Society of Mechanical Engineers, New York, 1993.
2. V.K. Gabrielson, "SHOCK, A Computer Code for Solving Lumped-Mass Dynamic Systems," Technical Report SCL-DR-65-34, Sandia Laboratories, Albuquerque, NM, 1966.
3. R.J. Fritz, "The Effect of Liquids on the Dynamic Motions of Immersed Solids," Journal of Engineering for Industry, Vol.94, pp.167-173, 1972.
4. M.J. Jhung, K.B. Park, "Dynamic Characteristics of Reactor Core for Pipe Break and Seismic Excitations, "KSME Journal, Vol. 6, No.2, pp.101-108, 1992.
5. USNRC, "Design Response Spectra for Seismic Design of Nuclear Power Plants," Regulatory Guide 1.60, US Nuclear Regulatory Commission, 1973.
6. E. Roos, et al., "Assessment of Large Scale Pipe Tests by Fracture Mechanics Approximation Procedures with Regard to Leak-Before-Break," Nuclear Engineering and Design, Vol.112, pp.183-195, 1989.
7. M.J. Jhung, et al., "Dynamic Analysis of Reactor Internals for the Tributary Pipe Breaks," Proceedings, 11th International Conference on SMiRT, Vol.J. Tokyo, August 1991.

APPENDIX

The coefficients for hydrodynamic mass matrix are defined in the forms for the four cases as follows :

1) outer cylinder fixed ; closed-open fluid annulus

$$m_{11}=\frac{16\rho aL^2}{\pi^2}\sum_{m=1,3}^{\infty}\frac{(-1)^{\frac{m-1}{2}}}{m^3\Delta}(\sin\frac{m\pi L_2}{2L}-\sin\frac{m\pi L_1}{2L})\{K_1'(\frac{m\pi b}{2L})I_1(\frac{m\pi a}{2L})-I_1'(\frac{m\pi b}{2L})K_1(\frac{m\pi a}{2L})\}$$

$$m_{12}=0$$

$$m_{21}=0$$

$$m_{22}=0$$

2) closed-open fluid annulus

$$m_{11}=\frac{16\rho aL^2}{\pi^2}\sum_{m=1,3}^{\infty}\frac{(-1)^{\frac{m-1}{2}}}{m^3\Delta}(\sin\frac{m\pi L_2}{2L}-\sin\frac{m\pi L_1}{2L})\{K_1'(\frac{m\pi b}{2L})I_1(\frac{m\pi a}{2L})-I_1'(\frac{m\pi b}{2L})K_1(\frac{m\pi a}{2L})\}$$

$$m_{12}=\frac{16\rho aL^2}{\pi^2}\sum_{m=1,3}^{\infty}\frac{(-1)^{\frac{m-1}{2}}}{m^3\Delta}(\sin\frac{m\pi L_2}{2L}-\sin\frac{m\pi L_1}{2L})\{-K_1'(\frac{m\pi a}{2L})I_1(\frac{m\pi a}{2L})+I_1'(\frac{m\pi a}{2L})K_1(\frac{m\pi a}{2L})\}$$

$$m_{21}=\frac{16\rho bL^2}{\pi^2}\sum_{m=1,3}^{\infty}\frac{(-1)^{\frac{m-1}{2}}}{m^3\Delta}(\sin\frac{m\pi L_2}{2L}-\sin\frac{m\pi L_1}{2L})\{-K_1'(\frac{m\pi b}{2L})I_1(\frac{m\pi b}{2L})+I_1'(\frac{m\pi b}{2L})K_1(\frac{m\pi b}{2L})\}$$

$$m_{22}=\frac{16\rho bL^2}{\pi^2}\sum_{m=1,3}^{\infty}\frac{(-1)^{\frac{m-1}{2}}}{m^3\Delta}(\sin\frac{m\pi L_2}{2L}-\sin\frac{m\pi L_1}{2L})$$

$$\{K_1'(\frac{m\pi a}{2L})I_1(\frac{m\pi b}{2L}) - I_1'(\frac{m\pi a}{2L})K_1(\frac{m\pi b}{2L})\}$$

$$m_{22} = 2\rho bL\sum_m \frac{h_m\int_{L1}^{L2} z_m(z)\,dz\, I_1(\frac{mb}{2L})}{mx_o I_1'(\frac{m\pi b}{2L})}$$

3) contained mass of an outer cylinder with no ineer cylinder

$$m_{11} = 0$$
$$m_{12} = 0$$
$$m_{21} = 0$$

4) outer cylinder fixed ; closed-closed fluid annulus.

$$m_{11} = \rho L\pi a^2 \left[\frac{b^2+a^2}{b^2-a^2}\right]$$
$$m_{12} = 0$$
$$m_{21} = 0$$
$$m_{22} = 0$$

(접수일자 : 1993. 4. 22)